ORIGINAL ARTICLE

Axisymmetric JKR-type adhesive contact under equibiaxial stretching

I. Argatov[a] and A. Papangelo[b,c]

[a]Malmö University, Department of Materials Science and Applied Mathematics, Bassänggatan 2, 21119 Malmö, Sweden; [b]University of Technology, Department of Mechanical Engineering, Am Schwarzenberg-Campus 1, 21073 Hamburg, Germany; [c]Politecnico di Bari, Department of Mechanics, Mathematics and Management, via Re David 200, 70125 Bari, Italy

ARTICLE HISTORY
Compiled June 14, 2019

ABSTRACT
An axisymmetric frictionless adhesive contact problem for a spherical indenter pressed against an isotropic elastic incompressible half-space under equibiaxial stretching is studied in the framework of the generalized Johnson–Kendall–Roberts (JKR) theory, which accounts for the effect of weak coupling between fracture modes I and II by means of a phenomenological mode-mixity function. The model predicts that contact area can withstand a larger level of the substrate stretch under moderate pre-pulling force. We have provided simple formulas to evaluate the pull-off force and the critical contact radius at the detachment point.

KEYWORDS
Adhesion; circular contact; incompressible substrate; fracture mode-mixity

1. Introduction

Adhesive contact has been frequently observed both in nature (Autumn & Puthoff, 2016; Vakis et al., 2018) and in industry (Popov, 2010), especially dealing with bio-inspired soft materials (Carbone, Pierro, & Gorb, 2011) and micro (nano) electromencahnical systems where surface forces plays a major role (Ciavarella & Papangelo, 2017).

A majority of studies (Borodich, 2014; Ciavarella, Joe, Papangelo, & Barber, 2019) consider normal contact under the external forces acting in the orthogonal direction to the contact interface, including the Johnson–Kendall–Roberts (JKR) theory (Johnson, Kendall, & Roberts, 1971) of axisymmetric adhesive elastic contact. It is known (Maugis, 2013) that the JKR theory is related to Griffith's energy-balance, which, in turn, can be characterized in terms of the mode I stress intensity factor (SIF), K_{I}, and its critical value, K_{Ic}.

The adhesive contact under the action of normal and tangential forces was considered as well (Johnson, 1996; Waters & Guduru, 2009; Mergel, Sahli, Scheibert, & Sauer, 2018; Sahli et al., 2018; Papangelo & Ciavarella, 2019; Sahli et al., 2019). In particular, the model of (Papangelo & Ciavarella, 2019) utilizes the mode II SIF, K_{II}, and takes into account the dependence of the interfacial toughness, G_{Ic}, on the ratio

$K_{\mathrm{II}}/K_{\mathrm{I}}$.

Recently, the effect of deformations induced by self-equilibrated loads acting parallel to the contact interface has been investigated both theoretically (Gay, 2000; Chen & Gao, 2005) and experimentally (Waters, Kalow, Gao, & Guduru, 2012). It has been shown that the generalized JKR model applies well for describing the evolution of the contact radius, provided the mode-mixity dependence of work of adhesion has been taken into account as follows:

$$\frac{K_{\mathrm{I}}^2 + K_{\mathrm{II}}^2}{K_{\mathrm{Ic}}^2} = f_{\mathrm{II}}(\psi_2). \tag{1}$$

Here, $f_{\mathrm{II}}(\psi_2)$ is the mode-mixity function (Hutchinson & Suo, 1991), and $\psi_2 = \arctan(K_{\mathrm{II}}/K_{\mathrm{I}})$ is the phase angle. We also recall that by standard LEFM arguments, we have $K_{\mathrm{Ic}} = \sqrt{2E^*G_{\mathrm{Ic}}}$, where E^* is the reduced elastic modulus, and G_{Ic} is the critical energy release rate for crack propagation.

In the present paper, we extend the analysis of (Waters et al., 2012) providing closed form solutions for critical strain and contact radius at the instability point. In the last section the model prediction are compared with the experimental data of (Waters et al., 2012) and, in particular, a practically interesting question of determining the mode-mixity function from experimental data is considered.

2. Axisymmetric adhesive contact under equibiaxial stretching

Let an incompressible elastic half-space be indented with an axisymmetric rigid probe, whose surface is determined by the equation

$$z = -\Phi(r), \tag{2}$$

where $\Phi(r)$ is a shape function, such that $\Phi(r) \geq 0$ and $\Phi(r) = 0$. Moreover, it is tentatively assumed that under the action of a normal load, P, the indenter establishes a circular contact area of radius a.

According to the Galin–Sneddon solution (Galin, 2008; Sneddon, 1965), the mode I SIF of the contact pressure is determined by the following formula (see, e.g., (Argatov & Mishuris, 2018)):

$$K_{\mathrm{I}} = \frac{E^*}{\sqrt{\pi}a^{3/2}} \int_0^a \frac{\Phi'(\rho)\rho^2\, d\rho}{\sqrt{a^2-\rho^2}} - \frac{P}{2\sqrt{\pi}a^{3/2}}. \tag{3}$$

Here, $E^* = E/(1-\nu^2)$ is the reduced elastic modulus; E and $\nu = 0.5$ are the substrate elastic modulus and Poisson's ratio, respectively.

At the same time, the indenter displacement is given by

$$\delta = \frac{P}{2E^*a} + \frac{1}{a}\int_0^a \frac{\Phi(\rho)\rho\, d\rho}{\sqrt{a^2-\rho^2}}. \tag{4}$$

In the case of a spherical punch of radius R, we have

$$\Phi(r) = \frac{r^2}{2R}, \tag{5}$$

and Eqs. (3) and (4) simplify as

$$K_{\mathrm{I}} = \frac{2E^* a^{3/2}}{3\sqrt{\pi}R} - \frac{P}{2\sqrt{\pi}a^{3/2}}, \tag{6}$$

$$\delta = \frac{P}{2E^* a} + \frac{a^2}{3R}. \tag{7}$$

Finally, equibiaxial stretch of the substrate induces the mode II SIF (see, e.g., (Aleksandrov, Smetanin, & Sobol, 1993; Waters et al., 2012))

$$K_{\mathrm{II}} = -2E^*\varepsilon\sqrt{\frac{a}{\pi}}, \tag{8}$$

where ε is the substrate equibiaxial strain.

The substitution of the SIFs K_{I} and K_{II} from Eqs. (7) and (8) into Eq. (1) yields the relation between the contact force P, the contact radius a, and the the substrate strain ε, which was derived previously (Waters et al., 2012). Observe that this model can be extended to the case of elastically similar materials, provided the elastic constant E^* is interpreted as the effective elastic modulus, while ε is defined as the mismatch strain.

In the case $\varepsilon = 0$, the outlined model (3) and (4) represents the generalization of the JKR theory developed previously (Borodich, Galanov, & Suarez-Alvarez, 2014; Maugis & Barquins, 1981; Zhou, Gao, & He, 2011).

3. Adhesive contact of a spherical probe and an elastic substrate under equibiaxial stretching

We consider a rigid indenter of radius R in no-slip contact with an incompressible elastic half-space, which is subsequently subjected to an equibiaxial strain ε (see Fig. 1). Under the action of a normal force, P, the indenter receives a vertical displacement, δ, and establishes a circular contact area of radius a, both of which, of course, also depend on the substrate stretch.

In what follows, we make use of the following dimensionless notation (Papangelo & Ciavarella, 2019):

$$\xi = \left(\frac{E^* R}{G_{\mathrm{Ic}}}\right)^{1/3}, \quad \tilde{a} = \frac{\xi a}{R}, \quad \tilde{\delta} = \frac{\xi^2 \delta}{R}, \quad \tilde{P} = \frac{P}{RG_{\mathrm{Ic}}}. \tag{9}$$

Here, $E^* = (4/3)E$ is the reduced elastic modulus of the incompressible substrate, and E is the substrate elastic modulus.

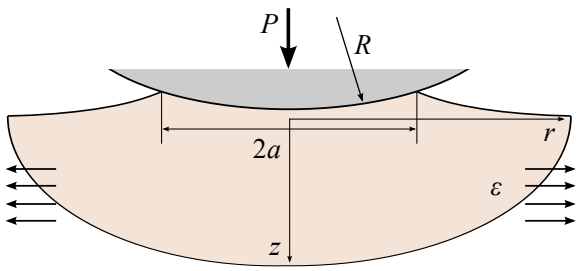

Figure 1. Schematic of the adhesive contact between a spherical probe and an elastic half-space under equibiaxial stretch.

In terms of the dimensionless variables $\tilde{P}$, $\tilde{\delta}$, and $\tilde{a}$, the LEFM based model (Waters et al., 2012) can be expressed as

$$\frac{2}{9\pi}\tilde{a}^3 + \frac{2\xi^2}{\pi}\varepsilon^2\tilde{a} + \frac{\tilde{P}^2}{8\pi\tilde{a}^3} - \frac{\tilde{P}}{3\pi} = f_{\mathrm{II}}(\psi_2), \tag{10}$$

where

$$\psi_2 = \arctan\frac{12\xi\varepsilon\tilde{a}^2}{3\tilde{P} - 4\tilde{a}^3}. \tag{11}$$

The dimensionless displacement of the spherical probe is given by

$$\tilde{\delta} = \frac{\tilde{P}}{2\tilde{a}} + \frac{\tilde{a}^2}{3}. \tag{12}$$

Observe that Eq. (10) involves three variables $\tilde{P}$, ε, and $\tilde{a}$. For given parameters of loading $\tilde{P}$ and ε, Eq. (10) with Eq. (11) being taken into account allows to determine the relative contact radius $\tilde{a}$.

In our analysis, we confine ourselves to the following one-parametric form of the mode-mixity (Hutchinson & Suo, 1991; Papangelo & Ciavarella, 2019):

$$f_b(\psi) = 1 + \tan^2[(1-\lambda)\psi]. \tag{13}$$

Here, $\lambda \in [0,1]$ is a mode-mixity parameter. It is readily seen that if $\lambda = 1$, we have $f_b(\psi) \equiv 1$, so that Eq. (1) reduces to the Griffith surface energy criterion of ideal brittle fracture. It is interesting to note that the limit case $\lambda \to 0$ is characterized by uncoupling of modes where everything depend on mode I (or, to be more precise, the fracture criterion (1) reduces to $K_{\mathrm{I}} = K_{\mathrm{Ic}}$).

We also note that as ψ tends to zero, the function (13) reveals a quadratic asymptotic approximation $1 + m\psi^2 + O(\psi^4)$, where the coefficient m depends on λ.

Finally, by setting $\varepsilon = 0$ in Eq. (10), we arrive at the equation

$$\frac{2}{9\pi}\tilde{a}^3 + \frac{\tilde{P}^2}{8\pi\tilde{a}^3} - \frac{\tilde{P}}{3\pi} = 1, \tag{14}$$

from where we recover relations of the JKR theory

$$\tilde{P}_{\mathrm{JKR}}(\tilde{a}) = \frac{4}{3}\tilde{a}^3 - \sqrt{8\pi\tilde{a}^3}, \tag{15}$$

$$\tilde{a}_{\mathrm{JKR}}(\tilde{P}) = \left(\frac{3}{4}\right)^{1/3}\left(3\pi + \tilde{P} \pm \sqrt{9\pi^2 + 6\pi\tilde{P}}\right)^{1/3}, \tag{16}$$

where the sign plus will be taken in what follows.

3.1. *Unstable detachment under tensile constant load and varying stretch*

Recall that according to the known stability analysis at fixed load (Maugis, 2013), the pull-off force $\tilde{P}_{\mathrm{c}}$ is determined by the condition that $d\tilde{a}/d\tilde{P}$ is infinite. In the adhesive contact problem under consideration, the equibiaxal stretch loading is applied under constant normal load, and therefore, we define the critical tensile force by the condition $d\tilde{a}/d\varepsilon$ is infinite. Hence, by differentiating Eq. (10) with respect to $\tilde{a}$, we arrive at the equation

$$3\tilde{a}^2 + 9\xi^2\varepsilon^2 - \frac{27}{16}\frac{\tilde{P}^2}{\tilde{a}^4} - \frac{9\pi}{2}f'_{\mathrm{II}}(\psi_2)\frac{\partial\psi_2}{\partial\tilde{a}} = 0, \tag{17}$$

where

$$\frac{\partial\psi_2}{\partial\tilde{a}} = \frac{24\tilde{a}\xi\varepsilon(2\tilde{a}^3 + 3\tilde{P})}{9\tilde{P} - 24\tilde{P}\tilde{a}^3 + 16\tilde{a}^6 + 144\tilde{a}^4\xi^2\varepsilon^2}. \tag{18}$$

The system of two equations (10) and (17) serves to define the critical characteristics $\tilde{a}_{\mathrm{c}}$ and $\tilde{P}_{\mathrm{c}}$ as a function of the stretch $\xi\varepsilon$.

Observe that in the case of "ideally brittle" fracture, when $f_{\mathrm{II}}(\psi_2) \equiv 1$, Eqs. (10) and (17) reduce to the problem of solving one algebraic equation

$$\tilde{a}_{\mathrm{c}}^3\left(\frac{\pi}{2} - \xi^2\varepsilon^2\tilde{a}_{\mathrm{c}}\right) = \left(\frac{3\pi}{4} - 2\xi^2\varepsilon^2\tilde{a}_{\mathrm{c}}\right)^2. \tag{19}$$

Thus, having determined $\tilde{a}_{\mathrm{c}}$ from Eq. (19) as a function of ε, we can substitute the result into Eq. (10) to obtain

$$\tilde{P}_{\mathrm{c}} = -\frac{4}{3}\tilde{a}_{\mathrm{c}}^2\sqrt{\tilde{a}_{\mathrm{c}}^2 + 3\xi^2\varepsilon^2}. \tag{20}$$

The above equation yields the critical tensile force for unstable detachment under constant load and varying stretch.

As a check, by setting $\varepsilon = 0$, we can recover the JKR pull-off force

$$\tilde{P}_{\mathrm{c,JKR}} = -\frac{4}{3}\tilde{a}_{\mathrm{c,JKR}}^3, \quad \tilde{a}_{\mathrm{c,JKR}} = \left(\frac{9\pi}{8}\right)^{1/3}.$$

The behavior of $\tilde{a}_{\mathrm{c}}$ and $\tilde{P}_{\mathrm{c}}$ as functions of $\xi\varepsilon$ is shown in Fig. 2.

From Fig. 2, it is readily seen that any stretch of an incompressible elastic substrate reduces the value of pull-off force.

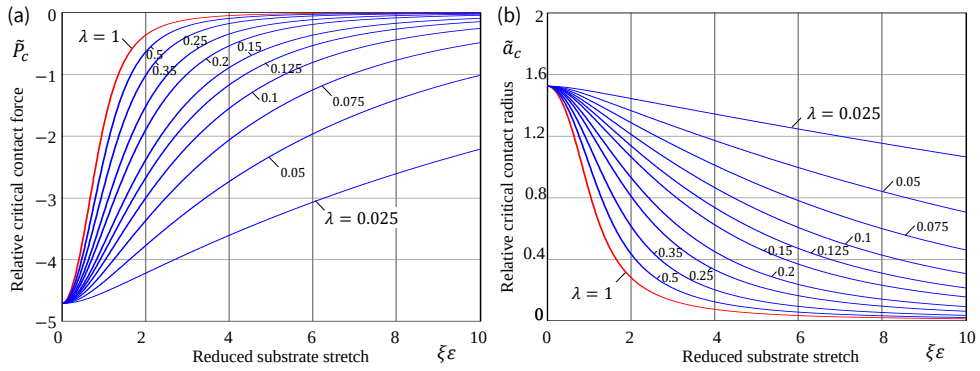

Figure 2. Influence of the substrate equibiaxial stretch on the critical tensile force (a) and the critical contact radius (b) in the case of model "b".

3.2. *Zero normal loading*

By setting $\tilde{P} = 0$ in Eqs. (11) and (10), we obtain

$$\psi_2 = -\arctan\frac{3\xi\varepsilon}{\tilde{a}}, \quad \frac{2}{9\pi}\tilde{a}^3 + \frac{2}{\pi}\xi^2\varepsilon^2\tilde{a} = f_{\mathrm{II}}(\psi_2). \tag{21}$$

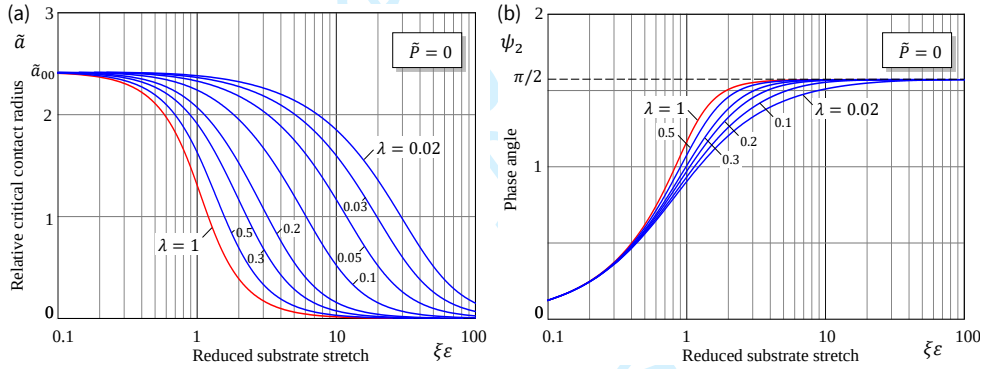

Figure 3. Variation of the contact radius (a) and the phase angle (b) as functions of the substrate equibiaxial stretch in the case of zero normal loading (model "b").

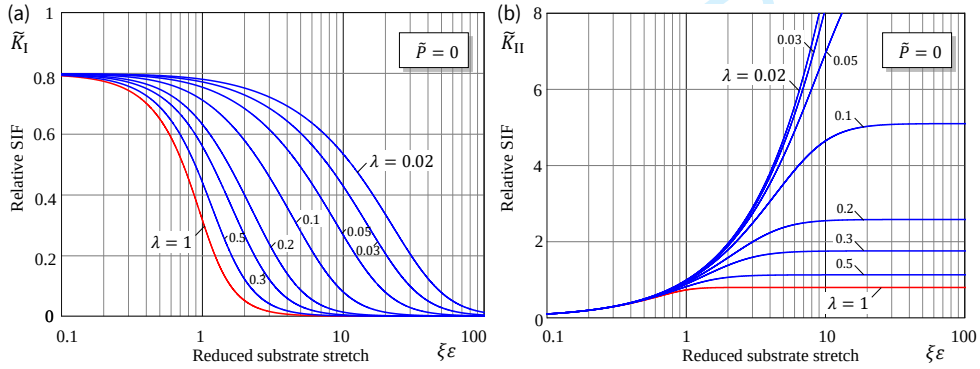

Figure 4. Variation of the stress intensity factors versus the substrate equibiaxial stretch in the case of zero normal loading (model "b").

In the case of "ideally brittle" fracture, when $f_{\rm II}(\psi_2) \equiv 1$, Eq. $(21)_2$ yields

$$\tilde{a} = \left(\sqrt{27(\xi\varepsilon)^6 + \frac{81\pi^2}{16}} + \frac{9\pi}{4}\right)^{1/3} - \left(\sqrt{27(\xi\varepsilon)^6 + \frac{81\pi^2}{16}} - \frac{9\pi}{4}\right)^{1/3}. \qquad (22)$$

The dimensionless variable $\tilde{a}$ as a function of $\xi\varepsilon$ is plotted in Fig. 3a (see the red line).

Using Eqs. (21), a graphical relation between $\tilde{a}$ and $\xi\varepsilon$ can be established (see Fig. 3a). It is readily seen that as ε increases, the contact radius $\tilde{a}$ decreases to zero from its initial value $\tilde{a}_{00} = \tilde{a}_{\rm JKR}(0)$ (see Eq. (16)). We note that $\tilde{a}_{00} = (9\pi/2)^{1/3} \approx 2.418$.

The behavior of dimensionless SIFs is shown Fig. 4. It interesting to observe that $\tilde{K}_{\rm II}$ tends to a constant value as $\xi\varepsilon$ goes to infinity, that is

$$\tilde{K}_{\rm II} \simeq \sqrt{\frac{2}{\pi} f_{\rm II}\Big(\frac{\pi}{2}\Big)}, \quad \xi\varepsilon \to \infty. \qquad (23)$$

This asymptotic value can be evaluated simply if we note that $\psi_2 \to \pi/2$ and $\tilde{a}(\xi\varepsilon)^2 \sim$ const as $\xi\varepsilon \to \infty$ (see Fig. 3b).

3.3. *Compressive normal loading*

Let $\tilde{P} > 0$ be kept constant. Then Eq. (10) can be solved for ε for given values of $\tilde{a}$ and ξ. As it was shown previously (Waters et al., 2012), ε increases as $\tilde{a}$ decreases (see Fig. 5a). However, it should be emphasized that the denominator in (11) approaches zero with increasing ε, thereby the phase angle ψ_2 tends to its critical value $\psi_2 = -\pi/2$. Therefore, a solution to Eq. (10) exists only for $\tilde{a} \in [\tilde{a}_0, \tilde{a}_{+\rm c})$, where $\tilde{a}_0 = \tilde{a}_{\rm JKR}(\tilde{P})$, and $\varepsilon \in [0, \varepsilon_{\rm c})$, such that

$$\tilde{a}_{+\rm c} = \Big(\frac{3}{4}\tilde{P}\Big)^{1/3}, \quad \xi^2\varepsilon_{\rm c}^2 = \frac{\pi}{2}\Big(\frac{4}{3}\Big)^{1/3}\tilde{P}^{-1/3} f_{\rm II}\Big(\frac{\pi}{2}\Big). \qquad (24)$$

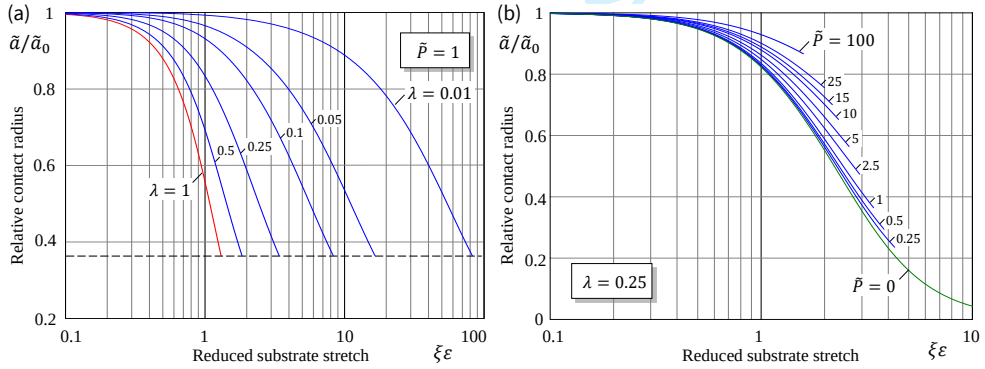

Figure 5. Predictions for the reduction in the relative contact radius versus the normalized mismatch strain in the case of compressive normal loading: (a) When the relative contact load $\tilde{P}$ is fixed (the dashed line is determined by Eq. $(24)_1$, which is obtained for vanishing $\tilde{K}_{\rm I}$); (b) When the parameter λ of the mode mixity function is fixed (model "b").

Observe that the second formula (24) shows that $\xi\varepsilon_{\rm c}$ increases unboundedly as $\tilde{P}$ tends to zero from the right (see Fig. 5b). For any fixed $\tilde{P} > 0$, the contact radius $\tilde{a}$ gradually decreases with the increase of the substrate stretch up to the moment when

$\tilde{K}_{\rm I}|_{\tilde{a}_0=\tilde{a}_{+c}} = 0$ where the curve stops. The limit curve is described by Eqs. (24) and is shown in Fig. 6b as the dot-dashed line.

3.4. *Tensile normal loading*

Now, we assume that $\tilde{P}$ is negative and $|\tilde{P}| < |\tilde{P}_{\rm c}|$, where $\tilde{P}_{\rm c}$ is defined by Eq. (19), (20) for a given value of ε. It is clear that if the strain ε is diminished, the originally established contact increases to that predicted by the JKR theory for $\varepsilon = 0$. If, then, for the same value of $\tilde{P}$, the strain ε starts to increase from zero, the contact radius will shrink to some critical value $\tilde{a}_{\rm c}$ which depends on both ε and $\tilde{P}$ (see Fig. 6).

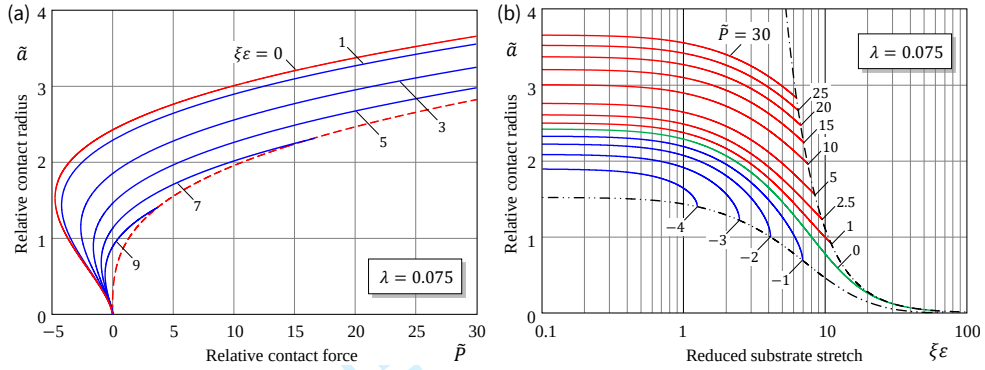

Figure 6. (a) Variation of the dimensionless contact radius $\tilde{a}$ as a function of the dimensionless contact force $\tilde{P}$ for different levels of the substrate equibiaxial stretch (the red solid and dashed lines correspond to the JKR and Hertzian solutions, respectively); (b) Variation of $\tilde{a}$ as a function of the reduced substrate equibiaxial stretch $\xi\varepsilon$ (the dot-dashed line is described by Eqs. (24), that is $\tilde{K}_{\rm I}|_{\tilde{a}=\tilde{a}_c} = 0$, while the double-dot-dashed line corresponds to the solution of Eqs.(10) and (17)), corresponding to the unstable detachment for the case of tensile contact load.

In other words, there is a critical value of ε beyond which higher stretch cannot be sustained by the contact interface without slip occurring (Waters et al., 2012).

4. Determining the mode-mixity function from experimental results

4.1. *Normalization of the contact radius/force equation*

We consider the case of equibiaxial stretching, which is described by Eqs. (11) and (10) in terms of the dimensionless variables $\tilde{a}$ and $\tilde{P}$ defined by Eqs. (9). Returning back to the physical variables a and P, we obtain

$$a^3 + 9\varepsilon^2 R^2 a + \frac{9R^2P^2}{16E^{*2}a^3} - \frac{3RP}{2E^*} - \frac{9\pi}{2}\frac{R^2 G_{\rm Ic}}{E^*} f_{\rm II}(\psi_2) = 0, \tag{25}$$

where

$$\psi_2 = \arctan\frac{12\varepsilon E^* R a^2}{3RP - 4E^* a^3}. \tag{26}$$

In the case $\varepsilon = 0$, Eqs. (26) and (25), respectively, reduce to $\psi_2 = \pi/2$ and the JKR

equation

$$a_0^3 + \frac{9R^2P^2}{16E^{*2}a_0^3} - \frac{3RP}{2E^*} - \frac{9\pi}{2}\frac{R^2G_{\mathrm{Ic}}}{E^*} = 0. \tag{27}$$

Now, following the previously used normalization (Chen & Gao, 2005), we introduce the dimensionless parameters

$$\hat{a} = \frac{a}{a_0}, \quad \hat{R} = \frac{R}{a_0}, \quad \hat{P} = \frac{3RP}{4E^*a_0^3}, \tag{28}$$

where a_0 satisfies Eq. (27).

The substitution of (28) into Eq. (27) yields the relation

$$\frac{9\pi\hat{R}^2G_{\mathrm{Ic}}}{2E^*a_0} = (1-\hat{P})^2. \tag{29}$$

On the other hand, substituting (28) into Eq. (25), we arrive at the equation

$$\hat{a}^3 + 9\varepsilon^2\hat{R}^2\hat{a} + \frac{\hat{P}^2}{\hat{a}^3} - 2\hat{P} - \frac{9\pi}{2}\frac{\hat{R}^2G_{\mathrm{Ic}}}{E^*a_0}f_{\mathrm{II}}(\psi_2) = 0, \tag{30}$$

where

$$\psi_2 = \arctan\frac{3\varepsilon\hat{R}\hat{a}^2}{\hat{P}-\hat{a}^3}. \tag{31}$$

Finally, by excluding G_{Ic} from Eq. (30) by means of Eq. (29), we obtain

$$\hat{a}^3 + 9\varepsilon^2\hat{R}^2\hat{a} + \frac{\hat{P}^2}{\hat{a}^3} - 2\hat{P} - (1-\hat{P})^2f_{\mathrm{II}}(\psi_2) = 0. \tag{32}$$

Note that, apart from notation and misprints, Eq. (32) corresponds to Eq. (7) derived previously (Waters et al., 2012).

4.2. *Determining the mode-mixity function*

Following the previously developed approach (Papangelo, Scheibert, Sahli, Pallares, & Ciavarella, 2019), we outline a procedure for determining the mode-mixity function $f_{\mathrm{II}}(\psi)$ from experimental data on adhesive contact under equibiaxial stretching.

As it has been pointed out previously (Waters et al., 2012), the mode I work of adhesion G_{Ic} can be determined using the JKR theory equation

$$G_{\mathrm{Ic}} = \frac{1}{8\pi E^*a_0^3}\left(\frac{4E^*a_0^3}{3R} - P\right)^2, \tag{33}$$

which is the same as Eq. (29).

Using the initial (for $\varepsilon = 0$) value of the contact radius a_0, the radius of a rigid probe R, the value of the contact force P, which remains constant, and the variable contact

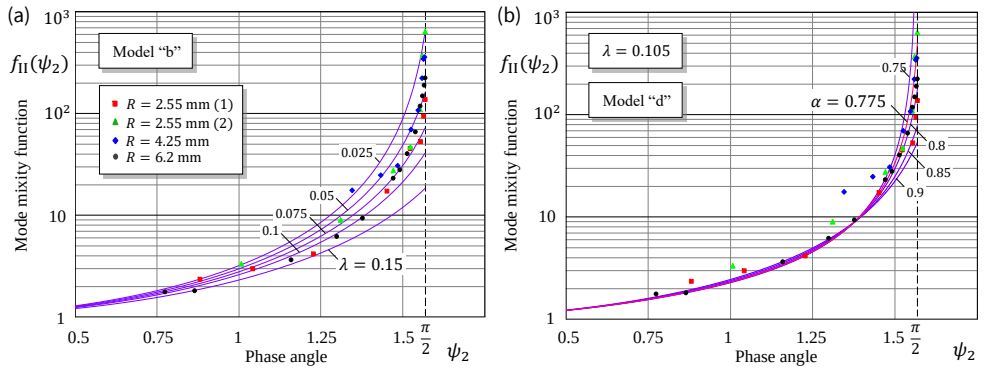

Figure 7. (a) Mode-mixity functions of the models "b" superimposed on the experimental data for equibiaxial stretching; (b) Mode-mixity function of the model "d" superimposed on the experimental data for equibiaxial stretching.

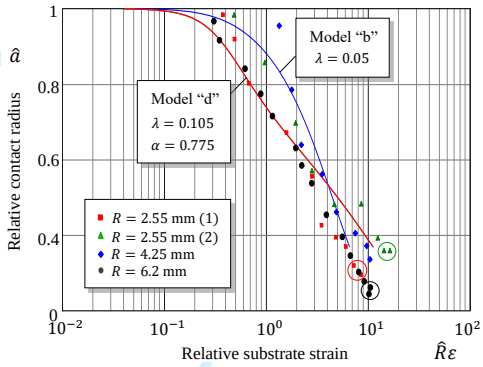

Figure 8. Experimental results (Waters et al., 2012) with fittings of the models "b" and "d".

radius a, which changes with the substrate strain ε, can be computed as defined in Eqs. (28). After that, formulas (31) and (32) allow to compute the phase angle ψ_2 and plot the values of $f_{II}(\psi_2)$ according to the equation

$$f_{II}(\psi_2) = \frac{1}{(1-\hat{P})^2}\left(\hat{a}^3 + 9\varepsilon^2\hat{R}^2\hat{a} + \frac{\hat{P}^2}{\hat{a}^3} - 2\hat{P}\right). \tag{34}$$

As an example, we consider the experimental data available in the literature (Waters et al., 2012) on stretching PDMS sheets in contact with a convex glass lens, whose weight provides a constant compressive normal load. The following data has been used to evaluate the experimental data: $R = 2.55$ mm, $P = 0.13$ mN, $G_{Ic} = 53$ mJ/m^2, $\hat{R} = 19$, and $\hat{P} = 0.05$.

Fig. 7a shows the experimentally evaluated predictions for the mode-mixity function and the analytical predictions according to the model "b". This observation reveals the importance of the behavior of $f_{II}(\psi)$ as ψ approaches $\pi/2$. We note that from (13), it follows that $f_b(\pi/2) = 1 + \tan^2[(1-\lambda)\pi/2] \simeq (4/\pi^2)\lambda^{-1}$, as $\lambda \to 0$.

It is clear that the fit can be improved by modifying the analytical expression for $f_{II}(\psi)$. In this way, the following form for the mode-mixity function can be suggested (it will be called the model "d"):

$$f_d(\psi) = 1 + \tan^{2\alpha}\left([(1-\lambda)\psi]^{1/\alpha}\right). \tag{35}$$

Observe that Eq. (35) differs from Eq. (13) by introducing an additional parameter α. In the case $\alpha = 1$, Eq. (35) reduces to Eq. (13). Moreover, for $\alpha > 0$, the asymptotic formula $f_d(\psi) \simeq 1 + (1-\lambda)^2\psi^2$ holds as $\psi \to 0$, which is the same as for $f_b(\psi)$.

Fig. 8a shows the results of the least-square fit of Eq. (35) to the experimental data (Waters et al., 2012) with the optimal values of the model parameters $\lambda = 0.105$ and $\alpha = 0.775$. Also, the dependency of the mode-mixity function on the parameter stirring is illustrated.

Fig. 8b presents the results of fitting of the developed phenomenological model (see Eqs. (31) and (32)) to the experimental data using two expressions for the mode-mixity function. It is of interest to note that some of the lower experimental points (which are encircled in the corresponding color) produced negative values of the phase angle.

5. Discussion

Let identify different loading scenarios, all of which include the initial stage of normal loading, when some circular contact area is established for a given of contact load. The first scenario is characterized by the subsequent stretching under a fixed relative normal load, $\tilde{P}_1 > 0$, up to the moment of unstable detachment (see Fig. 9a). It is emphasize that this critical state occurs when the mode I SIF vanishes, hence the Hertzian solution for the contact pressure is formally retrieved. We recall that the Hertzian contact pressure differs from that of the JKR model by the absence of any singularity at the boundary of the contact area.

The second scenario differs not only by the sign of relative normal load, $\tilde{P}_2 < 0$, but also by the mechanism of critical state when unstable detachment occurs (see Fig. 9a). Thus, the main difference between these two scenarios is that for tensile contact force $\tilde{P} < 0$ the substrate stretch leads to instability (see Figs. 2), whereas for compressive contact force $\tilde{P} > 0$ the subsequent substrate stretch diminishes the mode I SIF, i.e., $\tilde{K}_{\rm I} \to 0$.

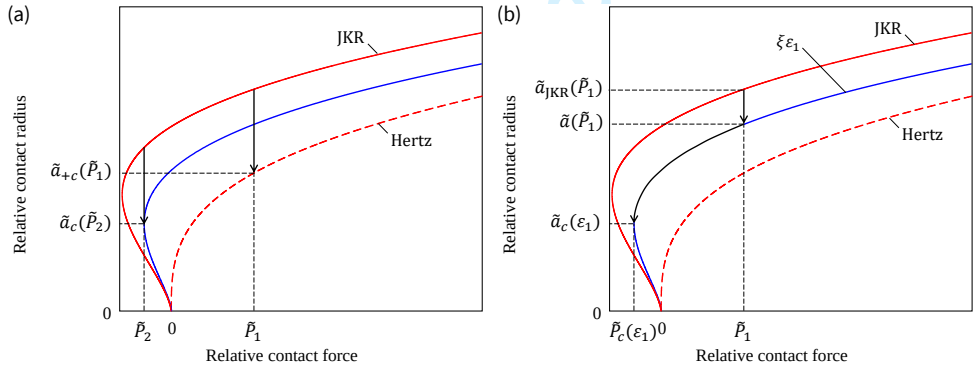

Figure 9. (a) First and second scenarios of stretch under a fixed normal load; (b) Third scenario of composite loading (see text for details).

The third scenario originates from the compressive JKR contact established for a certain relative contact force, $\tilde{P}_1 > 0$, and assumes the substrate stretch up to some value ε_1, which is below the corresponding critical level. During this loading stage, the relative contact radius decreases from the value $\tilde{a}_{\rm JKR}(\tilde{P}_1)$, which is predicted by the JKR model, to some value $\tilde{a}(\tilde{P}_1)$, which corresponds to the substrate strain ε_1. Finally, while fixing the substrate stretch, the contact force starts to decrease, thereby reaching the critical state at some value $\tilde{P}_{\rm c}(\varepsilon_1)$. The latter value of critical contact

force can be termed as the pull-off force. In other words, if we fix the stretch and then start unloading, we will get detachment at a certain contact radius $\tilde{a}_c(\varepsilon_1)$ like in the JKR theory but with different pull-off force $\tilde{P}_c(\varepsilon_1)$, since the substrate is stretched.

It is interesting to note that in the framework of the first scenario when $\tilde{P}_1 = 0$, the application of stretch doers not lead to any critical state with a finite substrate strain, but it can be said to be reached asymptotically for infinite stretch as $\varepsilon \to \infty$ (see Figs. 3). So, in this sense, in the case of zero contact loading, there is no critical substrate stretch (see also Fig. 4a).

6. Conclusions

In this work we have developed an approximate modeling framework for the JKR-type adhesive contact between a spherical indenter and an incompressible elastic substrate under equibiaxial uniform stretching. The validation of our model against experimental data has revealed that the least squares fitting is very sensitive to the choice of the mode-mixity function (Papangelo & Ciavarella, 2019). The model predicts the effect of strengthening of the contact interface by imposing a small pre-pulling force acting on the indenter, so that the contact area can withstand a larger level of the substrate stretching. We have provided general formulas (which depend on $f(\psi)$ explicitly) to obtain critical detachment force and contact radius (for constant strain), or critical stretch and contact radius (constant load).

7. Acknowledgment

The authors are indebted to Prof. M. Ciavarella for stimulating discussions. IA is grateful to the Teaching@Poliba program for the hospitality during his stay at the Polytechnic University of Bari, where this research was carried out. AP thanks Prof. M. Napolitano for his support with the "Center of excellence in computational mechanics" funding during year 2018. AP thanks the DFG (German Research Foundation) for funding the project PA 3303/1-1.

References

Aleksandrov, V., Smetanin, B., & Sobol, B. (1993). *Thin stress concentrators in elastic solids*. Nauka, Moscow (in Russian).

Argatov, I., & Mishuris, G. (2018). *Indentation testing of biological materials*. Cham: Springer.

Autumn, K., & Puthoff, J. (2016). Properties, principles, and parameters of the gecko adhesive system. In A. M. Smith (Ed.), *Biological adhesives* (pp. 245–280). Cham: Springer International Publishing.

Borodich, F. M. (2014). The hertz-type and adhesive contact problems for depth-sensing indentation. , *47*, 225–366.

Borodich, F. M., Galanov, B. A., & Suarez-Alvarez, M. M. (2014). The jkr-type adhesive contact problems for power-law shaped axisymmetric punches. *Journal of the Mechanics and Physics of Solids*, *68*, 14–32.

Carbone, G., Pierro, E., & Gorb, S. N. (2011). Origin of the superior adhesive

performance of mushroom-shaped microstructured surfaces. *Soft Matter*, *7*(12), 5545–5552.

Chen, S., & Gao, H. (2005). Non-slipping adhesive contact of an elastic cylinder on stretched substrates. *Proceedings of the Royal Society A: Mathematical, Physical and Engineering Sciences*, *462*(2065), 211–228.

Ciavarella, M., Joe, J., Papangelo, A., & Barber, J. (2019). The role of adhesion in contact mechanics. *Journal of the Royal Society Interface*, *16*(151), 20180738.

Ciavarella, M., & Papangelo, A. (2017). Discussion of "measuring and understanding contact area at the nanoscale: A review"(jacobs, tdb, and ashlie martini, a., 2017, asme appl. mech. rev., 69 (6), p. 060802). *Applied Mechanics Reviews*, *69*(6), 065502.

Galin, L. A. (2008). *Contact problems: the legacy of L.A. Galin* (G. M. L. Gladwell, Ed.). Dordrecht: Springer.

Gay, C. (2000). Does stretching affect adhesion? *International Journal of Adhesion and Adhesives*, *20*(5), 387–393.

Hutchinson, J. W., & Suo, Z. (1991). Mixed mode cracking in layered materials. In *Advances in applied mechanics* (Vol. 29, pp. 63–191). Elsevier.

Johnson, K. (1996). Continuum mechanics modeling of adhesion and friction. *Langmuir*, *12*(19), 4510–4513.

Johnson, K., Kendall, K., & Roberts, A. (1971). Surface energy and the contact of elastic solids. *Proceedings of the Royal Society of London. A. Mathematical and Physical Sciences*, *324*(1558), 301–313.

Maugis, D. (2013). *Contact, adhesion and rupture of elastic solids* (Vol. 130). Springer Science & Business Media.

Maugis, D., & Barquins, M. (1981). Adhesive contact of a conical punch on an elastic half-space. *Journal de Physique Lettres*, *42*(5), 95–97.

Mergel, J. C., Sahli, R., Scheibert, J., & Sauer, R. A. (2018). Continuum contact models for coupled adhesion and friction. *The Journal of Adhesion*, 1–33.

Papangelo, A., & Ciavarella, M. (2019). On mixed-mode fracture mechanics models for contact area reduction under shear load in soft materials. *Journal of the Mechanics and Physics of Solids*, *124*, 159–171.

Papangelo, A., Scheibert, J., Sahli, R., Pallares, G., & Ciavarella, M. (2019). *Shear-induced contact area anisotropy explained by a fracture mechanics model.* (accepted by Physical Review E)

Popov, V. L. (2010). *Contact mechanics and friction.* Heidelberg: Springer.

Sahli, R., Pallares, G., Ducottet, C., Ali, I. B., Al Akhrass, S., Guibert, M., et al. (2018). Evolution of real contact area under shear and the value of static friction of soft materials. *Proceedings of the National Academy of Sciences*, *115*(3), 471–476.

Sahli, R., Pallares, G., Papangelo, A., Ciavarella, M., Ducottet, C., Ponthus, N., et al. (2019). *Shear-induced anisotropy in rough elastomer contact.* (accepted by Physical Review Letters)

Sneddon, I. N. (1965). The relation between load and penetration in the axisymmetric boussinesq problem for a punch of arbitrary profile. *International Journal of Engineering Science*, *3*(1), 47–57.

Vakis, A., Yastrebov, V., Scheibert, J., Nicola, L., Dini, D., Minfray, C., et al. (2018). Modeling and simulation in tribology across scales: An overview. *Tribology International*, *125*, 169–199.

Waters, J. F., & Guduru, P. R. (2009). Mode-mixity-dependent adhesive contact of

a sphere on a plane surface. *Proceedings of the Royal Society A: Mathematical, Physical and Engineering Sciences*, *466*(2117), 1303–1325.

Waters, J. F., Kalow, J., Gao, H., & Guduru, P. R. (2012). Axisymmetric adhesive contact under equibiaxial stretching. *The Journal of Adhesion*, *88*(2), 134–144.

Zhou, S.-S., Gao, X.-L., & He, Q.-C. (2011). A unified treatment of axisymmetric adhesive contact problems using the harmonic potential function method. *Journal of the Mechanics and Physics of Solids*, *59*(2), 145–159.